Taylor & Francis
Taylor & Francis Group

Automatika

Journal for Control, Measurement, Electronics, Computing and Communications

ISSN: 0005-1144 (Print) 1848-3380 (Online) Journal homepage: http://www.tandfonline.com/loi/taut20

Fuzzy sliding mode control for erection mechanism with unmodelled dynamics

Jiangtao Feng, Qinhe Gao, Wenliang Guan & Xianxiang Huang

To cite this article: Jiangtao Feng, Qinhe Gao, Wenliang Guan & Xianxiang Huang (2017) Fuzzy sliding mode control for erection mechanism with unmodelled dynamics, Automatika, 58:2, 131-140, DOI: 10.1080/00051144.2017.1377913

To link to this article: https://doi.org/10.1080/00051144.2017.1377913

Published online: 26 Sep 2017.

AUTOMATIKA, 2017
VOL. 58, NO. 2, 131–140
https://doi.org/10.1080/00051144.2017.1377913

Taylor & Francis
Taylor & Francis Group

REGULAR PAPER

Fuzzy sliding mode control for erection mechanism with unmodelled dynamics

Jiangtao Feng, Qinhe Gao, Wenliang Guan and Xianxiang Huang

Xi'an High-Tech Research Institute, Xi'an, China

ABSTRACT

Erection mechanism is a complicated system suffering from nonlinearities, uncertainties and disturbances. It is difficult to establish mathematical model and perform a high precision control using linear control methods. In this study, adaptive fuzzy sliding mode control algorithm was designed to control erection mechanism. The proposed method combines the advantages of fuzzy logic and sliding mode control. The structure of the system is partially unknown and does not require the bounds of uncertainty to be known. Fuzzy logic is used to approximate the unknown parts of the system. The chattering phenomenon of sliding mode control is eliminated without deteriorating the system robustness. Experimental results of the position control under various reference trajectories are obtained. The proposed method can achieve favourable tracking performance for erection mechanism in the presence of unmodelled dynamics and disturbances.

ARTICLE HISTORY
Received 26 February 2017
Accepted 6 September 2017

KEYWORDS
Fuzzy logic control; sliding mode control; erection mechanism; electrohydraulic system

1. Introduction

Electrohydraulic proportional valve is adopted to control telescopic hydraulic cylinder for erection mechanism. The system is nonlinear and the dynamic characteristic is complex. The load of erection process is time-varying. It changes from positive to negative when passing the balance point. There is over-running load. Electrohydraulic open-loop and proportional–integral–derivative (PID) controllers are generally utilized to control erection process. Open-loop control methods are inherently stable, but are unable to deal with model uncertainties while PID controllers are mostly used to stabilize linear plants. Furthermore, in the case of time-varying plants with uncertainties guaranteeing stability using PID controller may be more demanding task. They have satisfactory control effect for linear and simple system and are widely used in industrial applications [1]. The open-loop control does not need feedback information of the system. PID controller works on the basis of the inputs of error, the derivative and the integral of error [2]. Classical PID control with fixed parameters cannot cope with time-varying nature of the plant in an optimal way. It is difficult to acquire great precision using them to control erection mechanism [3].

To improve the dynamics of nonlinear and uncertain system, numerous control strategies have been proposed to eliminating nonlinearities, uncertainties and disturbances. Many nonlinear controllers and adaptive control schemes have been proposed for hydraulic control systems, such as feedback linearization adaptive control, indirect adaptive control and nonlinear adaptive control based on backstepping techniques [4,5]. The increasing numbers of works involve linear control, nonlinear control and intelligent control methods. It is found that nonlinear control strategy has been an efficient approach [6]. Veysi [7] designed an optimal fuzzy sliding mode controller for controlling the end-effector position in the task space. Feedback linearization method and sliding mode control (SMC) were employed to overcome the uncertainties. Soltanpour [8] designed a sliding mode controller to control the position tracking of robot manipulator. The controller had global asymptotical stability in the presence of uncertainties and unmodelled dynamics. Yao [9] synthesized a robust integral of the sign of the error controller and an adaptive controller via backstepping method for motion control of a hydraulic rotary actuator. The controller guaranteed asymptotic tracking performance in the presence of various uncertainties. Fuzzy control using linguistic information possesses several advantages such as robustness, model-free and universal approximation theorem. Wang and Mendel [10,11] proposed that fuzzy logic systems were capable of uniformly approximating any nonlinear function. Fuzzy logic system is useful for plants having difficulties in deriving mathematical models. SMC has been given much attention by industrial and academic communities. It is usually utilized to control the systems facing uncertainty. It has advantages in having a simple structure and being robust against the parameter uncertainties [12]. The disadvantage of SMC is the chattering problem of control action due to its discontinuous switching part in

CONTACT Jiangtao Feng fengjt291082217@126.com

control law. Many researchers have tried to combine fuzzy logic and sliding mode method to achieve a better performance [13]. This integration approach is known as fuzzy sliding mode control. The application of fuzzy logic system to deal with the chattering problem is proven as an effective way [14].

Most of the control problems are usually solved by mathematical tools based on system model. But there are many complex processes whose accurate mathematical models are not available or difficult to formulate. One needs to handle uncertainties and nonlinearities in modelling such dynamic systems. The goal of this paper is to introduce an adaptive fuzzy SMC design for erection mechanism subject to uncertainties and disturbances. Fuzzy logic is able to approximate any real continuous system. Sliding mode controllers are robust to parameter variations and disturbance. In comparison with other approaches, the structure of system is partially unknown and does not require the bounds of uncertainty to be known in the presented method. The method is very useful when the precise model of the system under control in not available. The hybrid control strategy can guarantee the stability and robustness against disturbances caused by unmodelled dynamics.

2. Mathematical model of erection system

2.1. Mechanical analysis

Erection process is the moving process from horizontal state to vertical state driven by telescopic hydraulic cylinder, as shown in Figure 1.

The following equation can be obtained through Euler dynamic equations in coordinate system *oxy*:

$$J\boldsymbol{\theta}''(t) = \boldsymbol{F}_p(t)\cdot\overline{P_2P_4} - \boldsymbol{G}\cdot\overline{P_2P_5} \tag{1}$$

where J is the moment of inertia of load to point P_2, $\theta(t)$ is the erection angle, $\boldsymbol{F}_p(t)$ is the thrust force of hydraulic cylinder, $\boldsymbol{G}$ is the gravity of load.

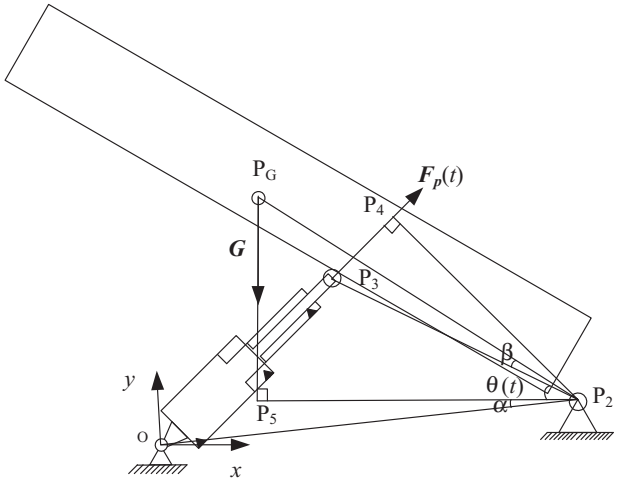

Figure 1. Erection diagram driven by telescopic cylinder.

Geometry relationships are described by the following equations:

$$\overline{P_2P_5} = \overline{P_2P_G}\cos(\theta(t)+\beta) \tag{2}$$

$$\overline{P_2P_4} = \overline{OP_2}\sin\angle P_2OP_3 = \overline{OP_2}\frac{\overline{P_2P_3}\sin(\theta(t)+\alpha)}{\overline{OP_3}} \tag{3}$$

$$\cos(\theta(t)+\alpha) = \frac{\overline{P_2P_3}^2 + \overline{OP_2}^2 - \overline{OP_3}^2}{2\overline{P_2P_3}\times\overline{OP_2}} \tag{4}$$

Thrust force of telescopic cylinder is obtained as follows:

$$|\boldsymbol{F_p}(t)| = \frac{\left[J|\boldsymbol{\theta}''(t)| + |\boldsymbol{G}|\cdot\overline{P_2P_G}\cos(\theta(t)+\beta)\right]\cdot\overline{OP_3}}{\overline{OP_2}\cdot\overline{P_2P_3}\cdot\sin(\theta(t)+\alpha)} \tag{5}$$

Figure 2(a) describes the relationship between erection angle and displacement of hydraulic cylinder. Figure 2(b) shows the relationship between thrust force

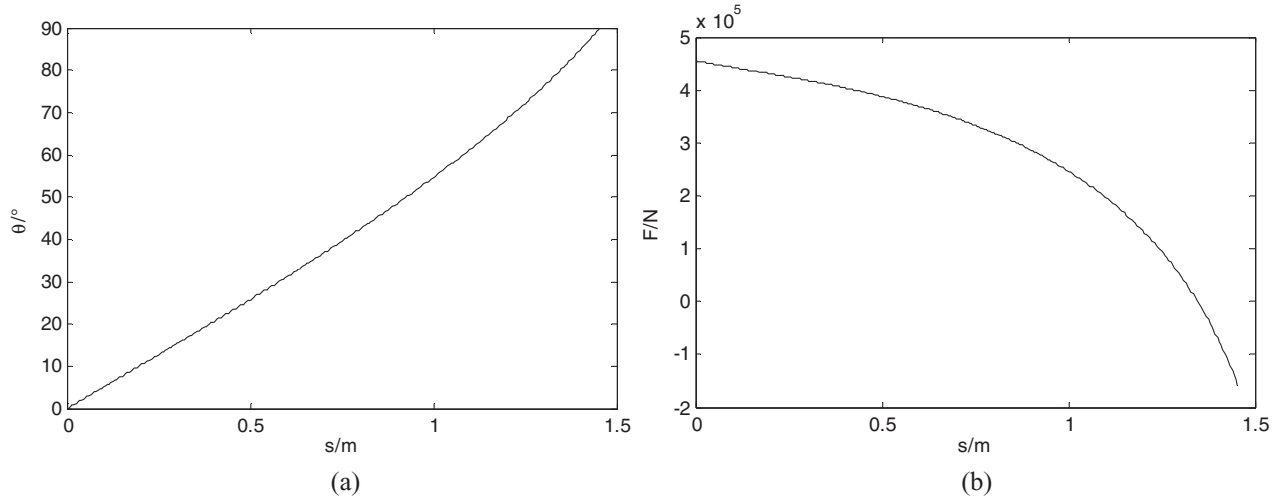

Figure 2. Erection angle and thrust force in erection process: (a) erection angle; (b) thrust force.

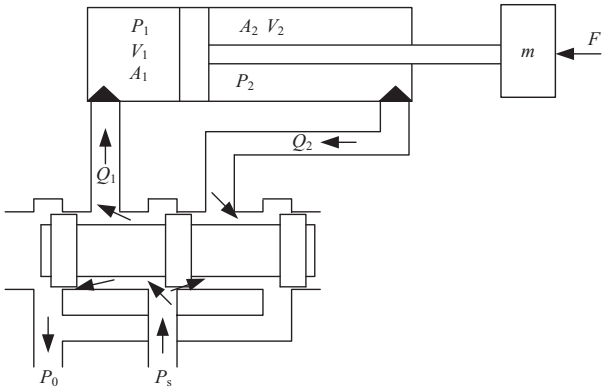

Figure 3. Schematic diagram of valve control hydraulic cylinder.

and displacement of hydraulic cylinder. Erection angle alters from 0° to 90° as the hydraulic cylinder extends from 0 to 1.5 m. The thrust force decreases gradually as hydraulic cylinder extends. It changes from positive to negative after the balance point. Thrust force is time-varying and there is negative value.

2.2. Valve control telescopic cylinder model

Schematic diagram of valve control hydraulic cylinder is shown in Figure 3.

The flow equation of proportional valve is a typical nonlinear equation. The flow formula is shown as follows:

$$Q_1 = \begin{cases} C_d w x_v \sqrt{2(P_S - P_1)/\rho} & x_v \geq 0 \\ C_d w x_v \sqrt{2P_1/\rho} & x_v < 0 \end{cases} \tag{6}$$

$$Q_2 = \begin{cases} C_d w x_v \sqrt{2P_2/\rho} & x_v \geq 0 \\ C_d w x_v \sqrt{2(P_S - P_2)/\rho} & x_v < 0 \end{cases} \tag{7}$$

where Q_1 and Q_2 represent the flow rates into piston chamber and out of piston rod chamber, C_d is the discharge coefficient, w is the area gradient of valve spool, x_v is the displacement of valve spool, P_s is the supply pressure, P_1 is the pressure of piston chamber, P_2 is the pressure of piston rod chamber.

The flow continuity equations of hydraulic cylinder are shown as follows:

$$Q_1 = A_1\dot{x}_p + C_i(P_1 - P_2) + \frac{V_1}{\beta_e}\dot{P}_1 \tag{8}$$

$$Q_2 = A_2\dot{x}_p + C_i(P_1 - P_2) - C_eP_2 - \frac{V_2}{\beta_e}\dot{P}_2 \tag{9}$$

where A_1 is the cross-sectional area of piston, A_2 is the annual area of piston rod, x_p is the displacement of piston rod, C_i is internal leakage coefficient, C_e is external leakage coefficient, V_1 and V_2 are volumes of piston and piston rod chambers, β_e denotes the effective bulk modulus.

Force equilibrium equation of piston is shown as follows:

$$\begin{aligned} &P_1A_1 - P_2A_2 \\ &= m\ddot{x}_p + B_c\dot{x}_p + Kx_p + |\boldsymbol{F}_p| + |\boldsymbol{F}_r| + |\boldsymbol{F}_d| \end{aligned} \tag{10}$$

where m is the equivalent mass of piston rod and load, B_c is the viscous damping coefficient of hydraulic cylinder, K is the elastic coefficient, $\boldsymbol{F}_p$ is external load, $\boldsymbol{F}_r$ is friction force, $\boldsymbol{F}_d$ is contact force of cylinder.

The friction force model between cylinders is defined as follows:

$$\begin{cases} \dfrac{dz}{dt} = |\boldsymbol{v}| - \dfrac{\sigma_a z}{g(\boldsymbol{v},h)}|\boldsymbol{v}|, \\ |\boldsymbol{F}_r| = \sigma_a z + \sigma_b\dfrac{dz}{dt} + \sigma_c|\boldsymbol{v}|, \\ g(\boldsymbol{v},h) = |\boldsymbol{F}_c| + [(1-h)|\boldsymbol{F}_s| - |\boldsymbol{F}_c|]e^{-(\boldsymbol{v}/v_s)^n}, \end{cases} \tag{11}$$

where z is the mean deformation of the bristles, $\boldsymbol{v}$ is the relative velocity of contact surfaces, σ_a is the stiffness of bristles, σ_b is the damping coefficient of bristles, σ_c is the viscous friction coefficient, $\boldsymbol{F}_c$ is Coulomb friction, h is the thickness of oil film, $\boldsymbol{F}_s$ is the static friction, v_s is Stribeck velocity constant.

The collision force is defined in the following formula:

$$|\boldsymbol{F}_d| = \begin{cases} K_p\delta^n + D_p\delta^m(|v_R| - |v_C|), & x \geq g_p; \\ 0, & g_n < x < g_p; \\ K_n\delta^n + D_n\delta^m(|v_R| - |v_C|), & x \leq g_n, \end{cases} \tag{12}$$

where K_p and K_n are effective spring stiffness, D_p and D_n are effective damping coefficient, δ is the normal penetration depth of contact point, v_R and v_C are speeds of two stage cylinders, x is relative displacement between piston and cylinder, g_p is the upper stroke, g_n is the lower stroke.

Define state variables $x_1 = x_p, x_2 = \dot{x}_p, x_3 = \ddot{x}_p$, x_1, x_2, x_3 are, respectively, the displacement, velocity, acceleration of piston rod. The system state equation is shown as follows. i represents the stage of hydraulic cylinder:

$$\begin{cases} \dot{x}_1 = x_2 \\ \dot{x}_2 = x_3 \\ \dot{x}_3 = a_{i1}x_2 + a_{i2}x_3 + g(x_v)u/a_{i3} + a_{i4} \end{cases} \tag{13}$$

where $g(x_v) = \begin{cases} \sqrt{(P_S - P_{iL})} & x_v \geq 0 \\ \sqrt{(n_i P_S + P_{iL})} & x_v < 0 \end{cases}$;

$a_{i1} = -\frac{\beta_e(1+n_i^2)}{m_i V_{i0}}\ (A_{i1}^2 + C_{it}B_{ic});\ a_{i2} = -\frac{B_{ic}}{m_i} - \frac{C_{it}\beta_e(1+n_i^2)}{V_{i0}};$

$a_{i3} = \frac{m_i V_{i0}}{A_{i1}\beta_e(1+n_i^2)C_d w k_p} / \sqrt{\frac{2}{\rho(1+n_i^3)}};\ a_{i4} = -\frac{\dot{F}+\dot{F}_r+\dot{F}_c}{m_i}$

$$-\frac{C_{it}\beta_e(1+n_i^2)}{m_i V_{i0}}(F + F_{ir} + F_{ic}) - \frac{A_{i1}\beta_e(1+n_i^2)}{m_i V_{i0}} b_i P_S$$

.

2.3. Unmodelled dynamics of electrohydraulic system

The electrohydraulic system is complex and its accurate model is hard to derive. Simplified model is often used in the analysis and design of control system. Unmodelled dynamics is unavoidable in practical control systems. The following assumptions are often made:

Assumption 2.1: *Oil temperature and effective bulk modulus are constant. Effective bulk modulus of mineral oil varies with pressure and temperature in actual process. The undissolved air mixed in hydraulic oil reduces its actual bulk modulus. One per cent of gas content reduces the actual bulk modulus to only about one-third. As the pressure increases, the amount of air dissolved in the hydraulic oil increases. The bulk modulus of undissolved air also increases due to compression. Figure 4 depicts the bulk modulus of HLP46 mineral oil under different pressures. The bulk modulus increases as pressure increase.*

Assumption 2.2: *Throttle window of zero-opening four-side valve is matching and symmetry. The flow rate–pressure equation of the valve is a linear equation* $Q = C_d w x_v \sqrt{2\Delta P/\rho}$.

The above formula is the flow rate formula through the thin wall hole under turbulence state. The size of the hole in practice generally cannot satisfy the required conditions of ideal thin wall hole. Flow coefficient changes with the different holes' shapes. Even the square root relationship is not necessarily able to meet. The flow rate formula of thin wall hole is often used to calculate the flow rate through slide throttle valve. The orifices of slide valve have a variety of shapes in practical application. Change of flow coefficient as flow number is shown in Figure 5.

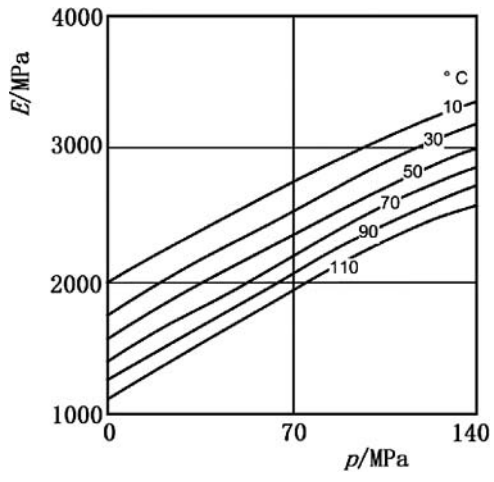

Figure 4. The bulk modulus of HLP46 mineral oil.

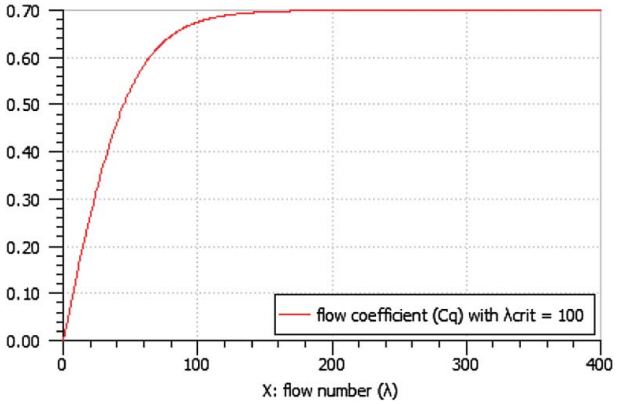

Figure 5. Change of flow coefficient as flow number.

Assumption 2.3: *Pressure loss and the influence of pipe are ignored. Pipe is always present in hydraulic systems. The stiffness of pipe also affects the actual bulk modulus of hydraulic fluid. The influence of thick wall steel pipe is little, but the impact of the hose is much greater. Figure 6 depicts a comparison test result. It can be seen that the actual bulk modulus of hydraulic oil in thick wall steel pipe rises from 700 to 2000 MPa when the working pressure rises from low pressure to 20 MPa. The actual bulk modulus of hydraulic oil in the hose rises from about 300 to 600 MPa, which is only about 1/3 of steel pipe.*

The liquid flowing in the pipe also results in pressure loss due to viscous friction. The pressure loss

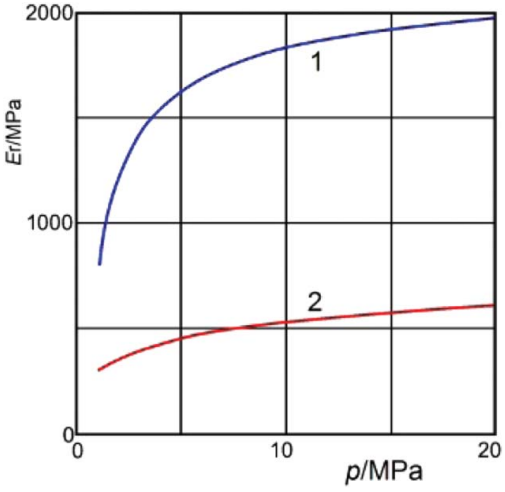

Figure 6. The measured bulk modulus of hydraulic oil in steel pipe and high-pressure hose (1 – steel pipe, outside diameter 30 mm, wall thickness 4 mm, length 3 m; 2 – high-pressure hose, inside diameter 30 mm, length 3 m) [15].

along the path in the equal diameter pipe is as follows:

$$\Delta p = \lambda \frac{l}{d} \frac{\rho v^2}{2}$$

where λ is the drag coefficient, which is related to pipe material, liquid flow state and so on, l is the pipe length, d is the pipe diameter, ρ is the fluid density, v is the average speed of fluid.

The speed and direction of the flow rate will change when liquid flows through the local resistance device (pipe elbow, pipe joint, a sudden change in the cross-section or valve port and so on). It will make the formation of local vortex and particle collisions between each other, resulting in pressure and kinetic energy loss. The flow state of the liquid through the above mentioned local devices is complicated and affected by many factors. It is difficult to analyse and calculate theoretically. Resistance coefficient ζ is generally measured rely on experiment. The pressure loss is calculated using the following formula $\Delta p = \zeta \frac{\rho v^2}{2}$.

By the analyses of the points above, the model based on these assumptions is not accurate. Therefore control strategy based on the model will results in a large error.

3. Adaptive fuzzy sliding mode control

SMC is robust to parameter variation but the accurate system function should be derived. Fuzzy logic system is capable of approximating any real continuous system [16,17]. Therefore, fuzzy sliding mode control (FSMC) is realized according to the logic rule designed based on experience. The model and disturbance are realized by using the universal approximation approach of fuzzy system. Adaptive FSMC without model information is realized by parameter adaptive adjustment.

3.1. Traditional sliding mode control

Consider the following third-order single-input–single-output (SISO) nonlinear system:

$$\dddot{x} = f(x,t) + g(x,t)u(t) + d(t) \tag{14}$$

where $f(x,t)$ and $g(x,t)$ are nonlinear functions, $d(t)$ is bounded external disturbance. $|d(t)| \le D, g(x,t) > 0$.

Defined switching function:

$$s(x,t) = k_1 e + k_2 \dot{e} + \ddot{e} \tag{15}$$

where k_1 and k_2 satisfy the Hurwitz polynomial condition.

SMC law is designed as follows:

$$u(t) = \frac{1}{g(x,t)}\left(-f(x,t) - k_1\dot{e} - k_2\ddot{e} + \dddot{x}_d - \eta \mathrm{sgn}(s)\right) \tag{16}$$

where $\eta \ge D$. Then,

$$\begin{aligned} \dot{s}(x,t) &= k_1\dot{e} + k_2\ddot{e} + \dddot{e} = k_1\dot{e} + k_2\ddot{e} + \dddot{x} \\ &- \dddot{x}_d = k_1\dot{e} + k_2\ddot{e} + f(x,t) + g(x,t)u(t) + d(t) - \dddot{x}_d \end{aligned} \tag{17}$$

The Lyapunov function is defined as $V = s^2/2$.

$$\dot{V} = s(x,t)\dot{s}(x,t) = d(x,t)s(x,t) - \eta\,|s(x,t)| \le 0 \tag{18}$$

The control law is not applicable when $f(x,t)$, $g(x,t)$ and the upper bound of $d(t)$ are unknown. So we use the fuzzy system $\hat{f}(x\,|\,\theta)$, $\hat{g}(x\,|\,\theta)$ and $\hat{h}(x\,|\,\theta)$ to approximate $f(x,t)$, $g(x,t)$ and $\eta\mathrm{sgn}(s)$.

3.2. Fuzzy approximation properties

Fuzzy system has universal approximation properties. Take $\hat{f}(x\,|\,\theta)$ approximation to $f(x,t)$ as an example. Five fuzzy sets are designed for the fuzzy system input x_1 and x_2, respectively. Take $n = 2$, $i = 1, 2$, $p_1 = p_2 = 5$, there are $p_1 \times p_2 = 25$ fuzzy rules. The following two steps are used to construct the fuzzy system $\hat{f}(x\,|\,\theta)$:

Step 1: Define p_i fuzzy sets for variable x_i $A_i^{l_i}$ ($l_i = 1, 2, 3, 4, 5$).

Step 2: Fuzzy rules $\prod_{i=1}^{n} p_i = p_1 \times p_2 = 25$ are used to construct fuzzy systems $\hat{f}(x\,|\,\theta)$. Then the jth fuzzy rule is in the following form:

$R^{(j)}$: IF x_1 is $A_1^{l_1}$ and x_2 is $A_2^{l_2}$ THEN $\hat{f}(x\,|\,\theta)$ is $B^{l_1 l_2}$, where $j = 1, 2, \ldots, 25$ and $B^{l_1 l_2}$ is the fuzzy set of the conclusion.

The fuzzy inference process uses the following four steps:

Step 1: Prerequisite reasoning is acquired based on product inference machine. The reasoning result is $\prod_{i=1}^{2} \mu_{A_i^{l_i}}(x_i)$.

Step 2: Use single-valued fuzzy for $\overline{y}_f^{\,l_1 l_2}$. That is the function $f(x_1,x_2)$ of the membership function corresponding to the maximum value.

Step 3: The product inference machine is used to realize reasoning of the rule premise and rule conclusion. The reasoning result is $\overline{y}_f^{\,l_1 l_2}\left(\prod_{i=1}^{2} \mu_{A_i^{l_i}}(x_i)\right)$. All the fuzzy rules are implemented and operated. The output of the fuzzy system is $\sum_{l_1=1}^{5}\sum_{l_2=1}^{5} \overline{y}_f^{\,l_1 l_2}\left(\prod_{i=1}^{2} \mu_{A_i^{l_i}}(x_i)\right)$.

Step 4: Using the average defuzzifier, the output of the fuzzy system is

$$\hat{f}(x\,|\,\theta) = \frac{\sum_{l_1=1}^{5}\sum_{l_2=1}^{5} \overline{y}_f^{\,l_1 l_2}\left(\prod_{i=1}^{2} \mu_{A_i^{l_i}}(x_i)\right)}{\sum_{l_1=1}^{5}\sum_{l_2=1}^{5}\left(\prod_{i=1}^{2} \mu_{A_i^{l_i}}(x_i)\right)} \tag{19}$$

Let $\bar{y}_f^{l_1 l_2}$ is a free parameter and put it in collection $\theta \in R^{(25)}$. The fuzzy basis vector $\xi(x)$ is introduced. Then,

$$\hat{f}(x \mid \theta) = \hat{\theta}_f{}^T \xi(x) \tag{20}$$

$$\xi_{l_1 l_2}(x) = \frac{\prod_{i=1}^{2} \mu_{A_i^{l_i}}(x_i)}{\sum_{l_1=1}^{5} \sum_{l_2=1}^{5} \left(\prod_{i=1}^{2} \mu_{A_i^{l_i}}(x_i) \right)} \tag{21}$$

Similarly,

$$\hat{g}(x \mid \theta) = \hat{\theta}_g{}^T \xi(x); \hat{h}(x \mid \theta) = \hat{\theta}_h{}^T \phi(x);$$

$$\phi(x) = \frac{\prod_{i=1}^{2} \mu_{A_i^{l_i}}(x_i)}{\sum_{l_1=1}^{3} \sum_{l_2=1}^{3} \left(\prod_{i=1}^{2} \mu_{A_i^{l_i}}(x_i) \right)} \tag{22}$$

The vectors $\hat{\theta}_f$, $\hat{\theta}_g$ and $\hat{\theta}_h$ vary according to the adaptive laws. The adaptive laws are designed as follows:

$$\hat{\theta}_f = r_1 s \xi(x); \hat{\theta}_g = r_2 s \xi(x) u; \hat{\theta}_h = r_3 s \phi(s) \tag{23}$$

The membership functions of $f(x)$ and $g(x)$ are defined as follows:

$$\mu_{NM}(x_i) = \exp\left[-((x_i + \pi/3)/(\pi/12))^2\right];$$
$$\mu_{NS}(x_i) = \exp\left[-((x_i + \pi/6)/(\pi/12))^2\right];$$
$$\mu_{NS}(x_i) = \exp\left[-(x_i/(\pi/12))^2\right];$$
$$\mu_{NS}(x_i) = \exp\left[-((x_i - \pi/6)/(\pi/12))^2\right];$$
$$\mu_{NM}(x_i) = \exp\left[-((x_i - \pi/3)/(\pi/12))^2\right]$$

The membership functions of $f(x)$ and $g(x)$ are depicted in Figure 7.

The membership functions of switching function are designed as follows:

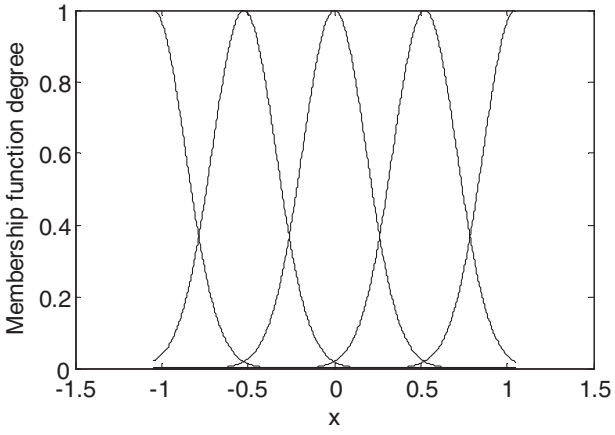

Figure 7. The membership functions of $f(x)$ and $g(x)$.

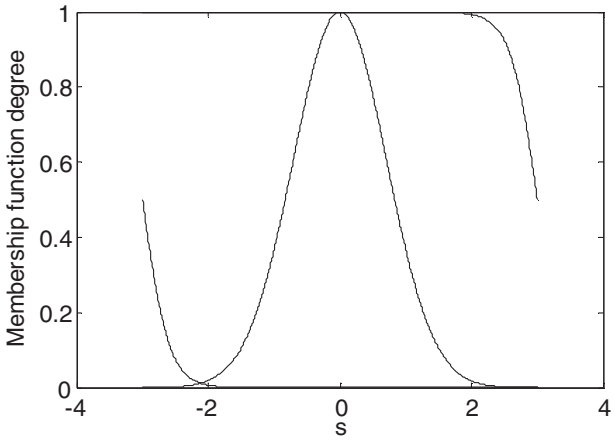

Figure 8. The membership functions of switching function.

$$\mu_N(s) = \frac{1}{1 + \exp(5(s+3))}; \mu_Z(s) = \exp(-s^2);$$
$$\mu_P(s) = \frac{1}{1 + \exp(5(s-3))}$$

The membership functions of switching function are depicted in Figure 8.

3.3. Adaptive fuzzy sliding mode control

The control law of FSMC is defined as follows:

$$u(t) = \frac{1}{\hat{g}(x,t)} \left(-\hat{f}(x,t) - k_1 \dot{e} - k_2 \ddot{e} + \dddot{x}_d - \hat{h}(s) \right) \tag{24}$$

The optimal parameters are defined as follows:

$$\theta_f^* = \arg\min[\sup |\hat{f}(x \mid \theta_f) - f(x,t)|] \tag{25}$$

$$\theta_g^* = \arg\min[\sup |\hat{g}(x \mid \theta_g) - g(x,t)|] \tag{26}$$

$$\theta_h^* = \arg\min[\sup |\hat{h}(s \mid \theta_h) - u_{sw}|] \tag{27}$$

The minimum approximation error is defined as $\omega = f(x,t) - \hat{f}(x \mid \theta_f^*) + (g(x,t) - \hat{g}(x \mid \theta_g^*))u(t)$.

Differentiating Equation (15) with respect to time,

$$\begin{aligned} \dot{s}(x,t) &= \sum_{i=1}^{n-1} k_i e^{(i)} + x^{(n)} - x_d{}^{(n)} \\ &= \sum_{i=1}^{n-1} k_i e^{(i)} + f(x,t) + g(x,t)u(t) + d(t) - x_d{}^{(n)} \\ &= \sum_{i=1}^{n-1} k_i e^{(i)} + f(x,t) + \hat{g}(x,t)u(t) + (g(x,t) \\ &\quad - \hat{g}(x,t))u(t) + d(t) - x_d{}^{(n)} \end{aligned}$$

$$
\begin{aligned}
&= f(x,t) - \hat{f}(x,t) - \hat{h}(s \mid \boldsymbol{\theta}_h) + (g(x,t) \\
&\quad - \hat{g}(x,t))u(t) + d(t) \\
&= \hat{f}(x \mid \theta_f^*) - \hat{f}(x,t) - \hat{h}(s \mid \boldsymbol{\theta}_h) + (\hat{g}(x \mid \theta_g^*) \\
&\quad - \hat{g}(x,t))u(t) + d(t) + \omega + \hat{h}(s \mid \boldsymbol{\theta}_h^*) - \hat{h}(s \mid \boldsymbol{\theta}_h^*) \\
&= \varphi_f^T \xi(x) + \varphi_g^T \xi(x) u(t) + \varphi_h^T \phi(x) + d(t) \\
&\quad + \omega - \hat{h}(s \mid \boldsymbol{\theta}_h^*)
\end{aligned}
$$

where $\varphi_f = \boldsymbol{\theta}_f^* - \boldsymbol{\theta}_f$, $\varphi_g = \boldsymbol{\theta}_g^* - \boldsymbol{\theta}_g$, $\varphi_h = \boldsymbol{\theta}_h^* - \boldsymbol{\theta}_h$. The Lyapunov function is defined as follows:

$$
V = \frac{1}{2}\left(s^2 + \frac{1}{r_1}\varphi_f^T \varphi_f + \frac{1}{r_2}\varphi_g^T \varphi_g + \frac{1}{r_3}\varphi_h^T \varphi_h\right) \tag{28}
$$

Differentiating Equation (28) with respect to time,

$$
\begin{aligned}
\dot{V} &= s\dot{s} + \frac{1}{r_1}\varphi_f^T \dot{\varphi}_f + \frac{1}{r_2}\varphi_g^T \dot{\varphi}_g + \frac{1}{r_3}\varphi_h^T \dot{\varphi}_h \\
&= s\Big(\varphi_f^T \xi(x) + \varphi_g^T \xi(x) u(t) + \varphi_h^T \phi(x) + d(t) \\
&\qquad + \omega - \hat{h}\big(s \mid \boldsymbol{\theta}_h^*\big)\Big) + \frac{1}{r_1}\varphi_f^T \dot{\varphi}_f + \frac{1}{r_2}\varphi_g^T \dot{\varphi}_g \\
&\qquad + \frac{1}{r_3}\varphi_h^T \dot{\varphi}_h \\
&= s\varphi_f^T \xi(x) + \frac{1}{r_1}\varphi_f^T \dot{\varphi}_f + s\varphi_g^T \xi(x) u(t) + \frac{1}{r_2}\varphi_g^T \dot{\varphi}_g \\
&\quad + s\varphi_h^T \phi(x) + \frac{1}{r_3}\varphi_h^T \dot{\varphi}_h + s\Big(d(t) - \hat{h}\big(s \mid \boldsymbol{\theta}_h^*\big)\Big) + s\omega \\
&= \frac{1}{r_1}\varphi_f^T \Big(r_1 s\xi(x) + \dot{\varphi}_f\Big) + \frac{1}{r_2}\varphi_g^T \Big(r_2 s\xi(x) u(t) + \dot{\varphi}_g\Big) \\
&\quad + \frac{1}{r_3}\varphi_h^T (r_3 s\phi(x) + \dot{\varphi}_h) + sd(t) + s\omega - (D + \eta) \mid s \mid \\
&= sd(t) + s\omega - (D + \eta) \mid s \mid \; \le s\omega - \eta \mid s \mid
\end{aligned}
$$

According to fuzzy approximation theory, adaptive fuzzy system can achieve approximation error w very small. Therefore, it can be guaranteed $\dot{V} \le 0$ by taking a large enough η. Then $s \equiv 0$ when $\dot{V} \equiv 0$. According to LaSalle invariant set principle, $t \to \infty$, $s \to 0$ [18].

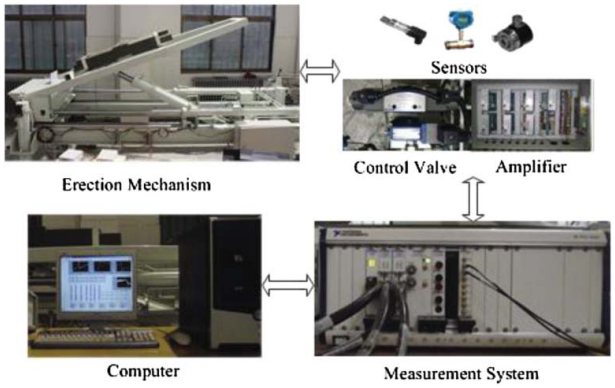

Figure 10. Experiment hardware of erection mechanism.

The control structure of FSMC is depicted in Figure 9. As shown, it uses two fuzzy inference approximators to construct the vectors $\xi(x)$ and $\phi(s)$. $\hat{f}(x \mid \theta)$, $\hat{g}(x \mid \theta)$ and $\hat{h}(x \mid \theta)$ are obtained to estimate the unknown functions $f(x,t)$, $g(x,t)$ and $\eta\mathrm{sgn}(s)$. The fuzzy approximator is applied to the sliding mode control.

4. Experimental results

Experimental hardware of erection mechanism is shown in Figure 10. The sensors are used to acquire the signals of pressure, displacement, erection angle and flow rate. The amplifier is utilized to control the electrohydraulic valve. NI PXI-6259 acquisition card is chosen as measurement system. Acquisition and control procedures are written using LabVIEW software. Main parameters of erection system are shown in Table 1.

The goal of the controller is to get the electrohydraulic system tracking the desired position references. FSMC, SMC and PID controllers are adopted to control the erection mechanism, respectively. Figure 11 shows the experiment results using a square wave

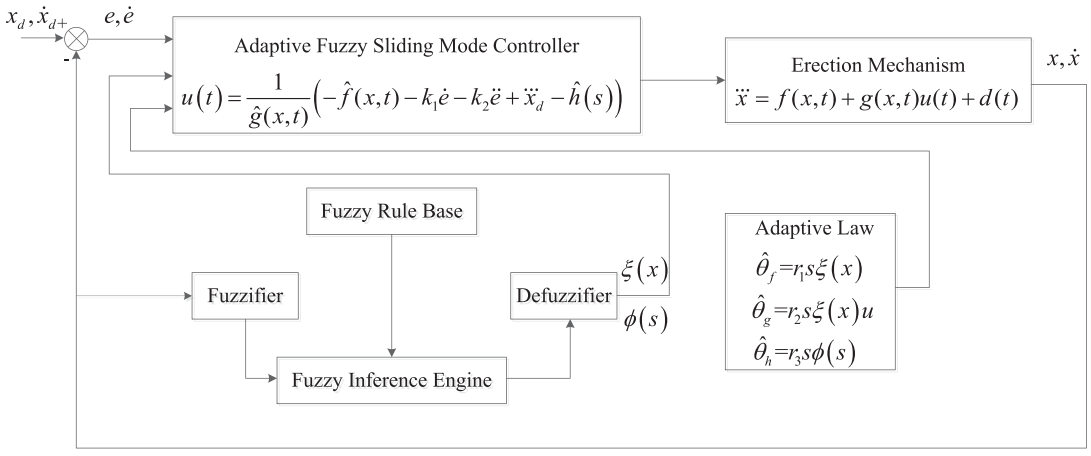

Figure 9. Control structure of FSMC.

Table 1. Main parameters of erection system.

Parameters	Values
Piston area of first stage A_{f1}/m^2	0.0314
Annular area of first stage A_{d1}/m^2	0.0031
Piston area of second stage A_{f2}/m^2	0.0177
Annular area of second stage A_{d2}/m^2	0.0133
Gravity of load G/N	147000
Moment of inertia J/Kg·m^2	133437
Stroke of first stage cylinder l_1/m	0.78
Stroke of second stage cylinder l_2/m	0.67
Mass of piston rod m/kg	178.31
Internal leakage coefficient $C_i/(m^3/s{\cdot}Pa)$	2.41×10^{-13}
External leakage coefficient $C_e/(m^3/s{\cdot}Pa)$	7.58×10^{-15}
Initial volume of cylinder V_0/m^3	1.7×10^{-5}
Supply pressure P_s/MPa	25
Flow coefficient C_d	0.62
Area gradient of valve w/m	2.51×10^{-2}
Bulk modules β_e/Pa	1.7×10^{9}
Fluid density $\rho/(kg/m^3)$	850
Constant k_1	5
Constant k_2	10

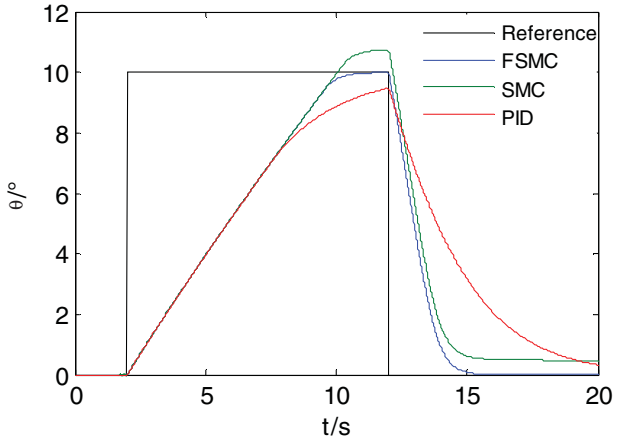

Figure 11. Responses of the controllers to a square wave reference trajectory.

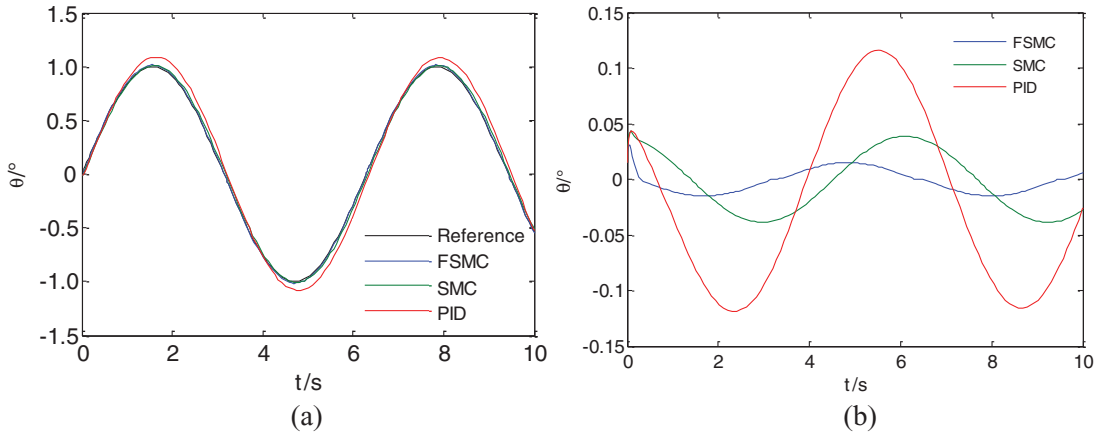

Figure 12. Responses of the controllers to a triangular wave reference trajectory: (a) response of the controllers; (b) position tracking error.

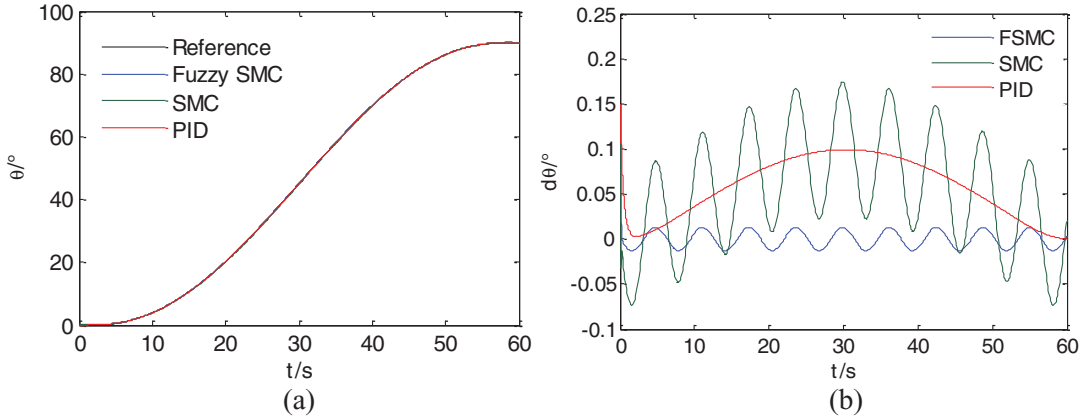

Figure 13. Erection angle controlled by different controllers: (a) erection angle; (b) position tracking error.

reference input. The position tracking is realized with the same rate at forward and backward motions of the cylinder. The response of FSMC has a much smaller overshoot and a shorter settling time.

Figure 12 presents the response and position tracking error of the controllers to a sinusoidal reference

Table 2. The maximum tracking errors of different controllers.

The maximum tracking error/°	FSMC	SMC	PID
Square wave	0.005	0.74	0.53
Triangular wave	0.03	0.05	0.12
Erection process	0.01	0.18	0.15

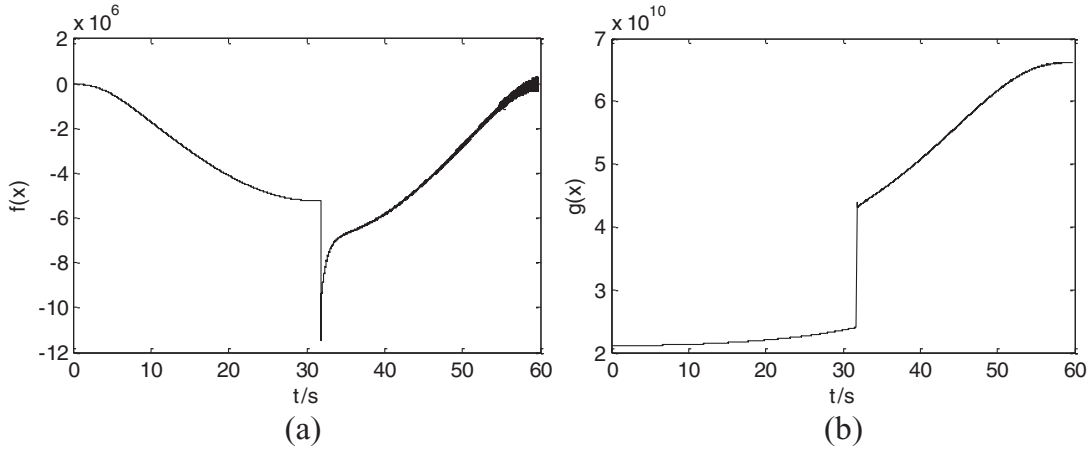

Figure 14. Approximation of $f(x)$ and $g(x)$ by fuzzy system: (a) approximation of $f(x)$; (b) approximation of $g(x)$.

trajectory. The result obtained with FSMC controller is in good agreement with the input compared to SMC and PID controllers. The FSMC controller clearly outperforms other controllers.

Figure 13 depicts the erection angle and tracking error. The control precision of traditional SMC is not high because of unmodelled dynamics. The position tracking performance of FSMC controller is better than SMC and PID controllers.

Table 2 depicts the maximum tracking errors of different controllers responding to square wave, triangular wave and erection process. It can be obtained from the table that the tracking error of FSMC controller is the least compared with SMC and PID controllers.

Figure 14 demonstrates the approximations of $f(x)$ and $g(x)$ by fuzzy system. The values of $f(x)$ and $g(x)$ have mutations when telescopic cylinder changes stage.

Figure 15 depicts the displacements of hydraulic cylinder. Figure 16 shows the pressure and flow rate of piston chamber and piston rod chamber. Two cylinder stages start to extend synchronously. When the first stage extends to the end of its stoke, the second stage continues to extend. The pressure in piston chamber decreases when each stage extends. It increases when the first stage extends to the end of its stroke. The pressure in piston rod chamber increases to balance the gravity when the second stage extends. The flow rate in piston chamber decreases and the flow rate in piston rod chamber increases when the first stage extends to its end stroke.

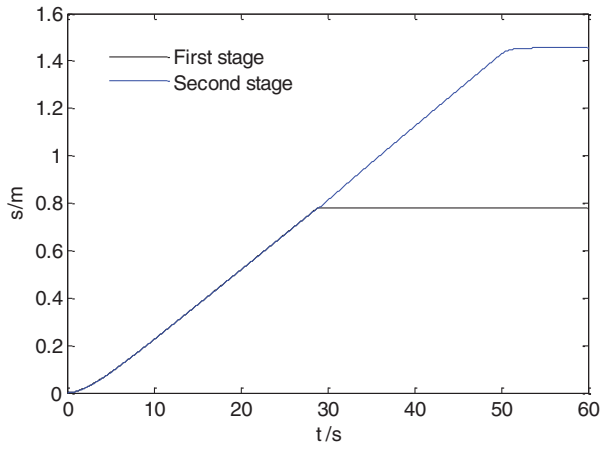

Figure 15. Displacements of two cylinder stages.

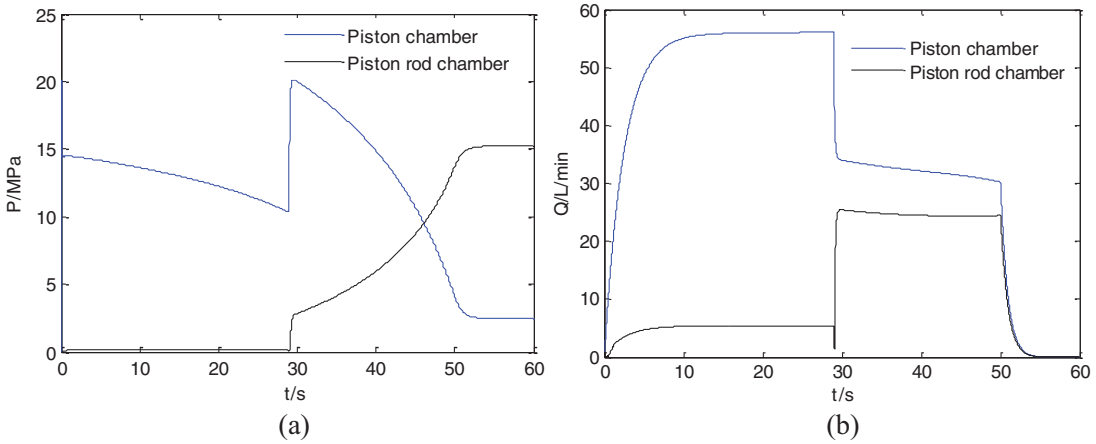

Figure 16. Pressure and flow rate curves in two chambers: (a) pressure curves; (b) flow rate curves.

5. Conclusions

In this paper, an adaptive fuzzy sliding mode controller is proposed for erection mechanism. The main idea of the proposed method is combination of fuzzy logic and traditional SMC. This approach takes the advantages of robustness of SMC and chattering elimination of fuzzy logic. Experiment results prove that the presented method improves tracking performance with smaller error in comparison with SMC and PID controllers. The research object of this paper is SISO erection system. This control strategy can be applied in multi-input–multi-output system in further developments. The algorithm can be applied to other industrial electro-hydraulic control systems, such as dump trucks, excavators and so on. There are some interesting issues as further works: decreasing computational burden of the control input; optimizing parameters of the control strategy; considering other challenges of hydraulic actuation systems, such as force/torque control.

Disclosure statement

No potential conflict of interest was reported by the authors.

Funding

This research was financially supported by the National Natural Science Foundation of China [grant number 51475462].

References

[1] Truong DQ, Ahn KK. Force control for hydraulic load simulator using self-tuning grey predictor – fuzzy PID. Mechatronics. 2009;19(2):233–246.
[2] Das S, Pan I, Das S, et al. A novel fractional order fuzzy PID controller and its optimal time domain tuning based on integral performance indices. Eng Appl Artif Intel. 2012;25(2):430–442.
[3] Pratumsuwa P, Thongchai S, Tansriwong S. A hybrid of fuzzy and proportional-integral-derivative controller for electro-hydraulic position servo system. Energy Res J. 2010;1(2):62–67.
[4] Kaddissi C, Kenné JP, Saad M. Indirect adaptive control of an electrohydraulic servo system based on nonlinear backstepping. IEEE/ASME Trans Mechatron. 2011;16(6):1171–1177.
[5] Mohanty A, Yao B. Indirect adaptive robust control of hydraulic manipulators with accurate parameter estimates. IEEE Trans Contr Syst Technol. 2011;19(3):567–575.
[6] Lei JB, Wang XY, Pi YJ. Sliding mode control in position control for asymmetrical hydraulic cylinder with chambers connected. J Shanghai Jiaotong Univ (Sci). 2013;18(4):454–459.
[7] Veysi M, Soltanpour MR, Khooban MH. A novel self-adaptive modified bat fuzzy sliding mode control of robot manipulator in presence of uncertainties in task space. Robotica. 2015;33(10):2045–2064.
[8] Soltanpour MR, Otadolajam P, Khooban MH. Robust control strategy for electrically driven robot manipulators: adaptive fuzzy sliding mode. Sci Meas Technol IET. 2015;9(3):322–334.
[9] Yao JY, Jiao ZX, Ma DW, et al. High-accuracy tracking control of hydraulic rotary actuators with modeling uncertainties. IEEE/ASME Trans Mechatron. 2014;19(2):633–641.
[10] Wang LX. Fuzzy systems are universal approximators. IEEE International Conference on Fuzzy Systems. IEEE Xplore. 1992;7:1163–1170.
[11] Wang LX, Mendel JM. Fuzzy basis functions, universal approximation, and orthogonal least-squares learning. IEEE Trans Neural Netw. 1992;3(5):807–814.
[12] Khooban MH, Niknam T, Blaabjerg F, et al. Free chattering hybrid sliding mode control for a class of nonlinear systems: electric vehicles as a case study. IET Sci Meas Technol. 2016;10(7):776–785.
[13] Khooban MH, Niknam T, Sha-Sadeghi M. A time-varying general type-II fuzzy sliding mode controller for a class of nonlinear power systems. IFS. 2016;30(30):2927–2937.
[14] Alfi A, Kalat AA, Khooban MH. Adaptive fuzzy sliding mode control for synchronization of uncertain non-identical chaotic systems using bacterial foraging optimization. J Intell Fuzzy Syst. 2014;26:2567–2576.
[15] Zhang HP. Hydraulic velocity control technology. Beijing: China Machine Press; 2014.
[16] Khanesar MA, Kaynak O, Yin S, et al. Adaptive indirect fuzzy sliding mode controller for networked control systems subject to time-varying network-induced time delay. IEEE Trans Fuzzy Syst. 2015;23(1):205–214.
[17] Soltanpour MR, Khooban MH, Khalghani MR. An optimal and intelligent control strategy for a class of nonlinear systems: adaptive fuzzy sliding mode. J Vib Control. 2016;22(1):159–175.
[18] Liu JK. Sliding mode control design and MATLAB simulation the basic theory and design method. 3rd ed. Beijing: Tsinghua University Press; 2012.